LA-UR-10- 10-07386

Approved for public release; distribution is unlimited.

Title: Electron Beam Radiography: a Proposed Plasma Diagnostic

Author(s):
Erik Vold
Frank Merrill
Eric Nelson
Fred Wysocki

Intended for: APS Division of Plasma Physics
Annual Meeting, Chicago, IL
November, 2010

Los Alamos
NATIONAL LABORATORY
EST. 1943

Los Alamos National Laboratory, an affirmative action/equal opportunity employer, is operated by the Los Alamos National Security, LLC for the National Nuclear Security Administration of the U.S. Department of Energy under contract DE-AC52-06NA25396. By acceptance of this article, the publisher recognizes that the U.S. Government retains a nonexclusive, royalty-free license to publish or reproduce the published form of this contribution, or to allow others to do so, for U.S. Government purposes. Los Alamos National Laboratory requests that the publisher identify this article as work performed under the auspices of the U.S. Department of Energy. Los Alamos National Laboratory strongly supports academic freedom and a researcher's right to publish; as an institution, however, the Laboratory does not endorse the viewpoint of a publication or guarantee its technical correctness.

Form 836 (7/06)

Electron Beam Radiography: a Proposed Plasma Diagnostic

Frank Merrill, P-25
Fred Wysocki, P-24
Erik Vold**, XCP-2
Eric Nelson , XCP-8
Los Alamos National Laboratory

** Presentation to American Physical Society
Division of Plasma Physics
Annual Meeting, Nov. 10, 2010

Electron Beam Radiography as a Proposed Plasma Diagnostic

Frank Merrill, P-25, Fred Wysocki, P-24, Erik Vold**, XCP-2, Eric Nelson , XCP-8
Los Alamos National Laboratory

Abstract

- Several recent studies have shown that charged particle diagnostics of ICF implosions provide new and useful information on the capsule implosion and the E and/or B fields associated with the finite scale plasma structures. Possible mechanisms for the plasma self-generation of these fields have been discussed but are not fully clear. In the present study, an electron beam (eBeam) radiography system (30MeV) is proposed which may have significant advantages over the existing methods which use 15 MeV nuclear-fusion driven protons as the charged particle diagnostic 'point' source. The relativistic electron beam has a greater penetration (cm2/g) and is predicted to have improved deflection from E or B relative to the scattering from multiple coulomb collisions. The scattering determines the plasma density image but simultaneously contributes noise to the signal due to E or B deflections. On-going studies focus on the forward calculation of the eBeam through simple plasma and test objects. The self-consistent generation of the E or B fields in the dynamic transient plasma may require new computational tools to explicitly include multi-species plasma in the presence of E or B fields and to resolve the mixing structures at the fuel-capsule interface in ICF implosions.

** Erik Vold presenter to APS DPP.

A proposed LANL diagnostic for NIF & other HED experiments

- For many laser-driven implosion experiments, a common desire is a measurement of the radial trajectory of shock-fronts in the fuel
  - Inward shock toward center
  - Reflected outgoing shock
  - Shock-front associated with E field in plasma regime
- Unstable material interfaces (e.g., capsule-fuel in ICF) in the presence of small scale 'mixing' structures are difficult to resolve
  - Expected to be associated w/ E and B fields
- These areas represent gaps in our present diagnostic capability
- A "new" diagnostic, if developed and deployed at large laser facilities (*e.g.*, NIF), could potentially fill this gap
  - Electron Radiography (eRad)
- This diagnostic compliments and builds on existing LANL expertise in charged particle radiography

Project Overview

- **Present and Near Term Scope**
  - Estimate densities, E and B fields from computations in inertial confinement and transient plasmas
  - Forward calculations of electron beam transport through test plasma objects and through a magnetic lens imaging system
  - Distinguish electron beam (eRad) signals due to MCS (multiple coulomb scatter) related to plasma rho-r from E & B deflection related to self-consistent plasma fields
  - Optimize magnetic lens / imaging to separate E and B and MCS signals

- **Longer Term Goals**
  - Promote and generate interest in eBeam radiography as a useful plasma diagnostic
  - Develop hardware / diagnostic capability for plasma and HEDP fluid dynamic structures
  - Improve understanding of E and B field generation in inertial confinement and transient plasmas, and their roles in transport and plasma fluid mixing.

MOTIVATION: The benefit of charged particle radiography has been demonstrated at Omega with fusion generated protons

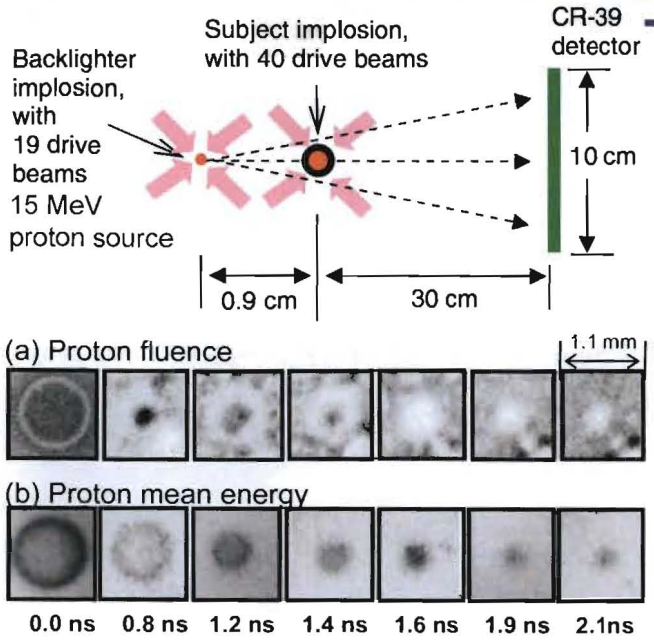

- A variety of information has been extracted from these data, *e.g.*,
  - Capsule radial trajectory
  - Total ρR vs time
  - Internal electric field due to fuel shocks
- A shock produces large ∇P_e and thus large E through the generalized Ohms law $E \approx -\nabla P_e / (e\, n_e)$ (in the absence of J and B)
- Charged particle radiography detects the large E, and thus the shock

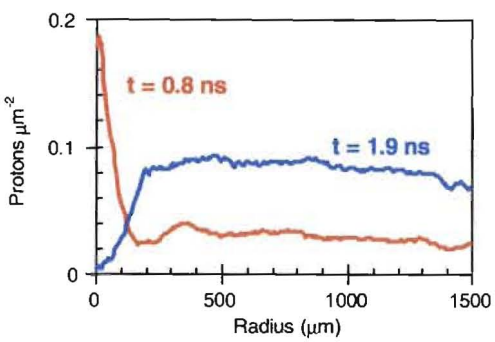

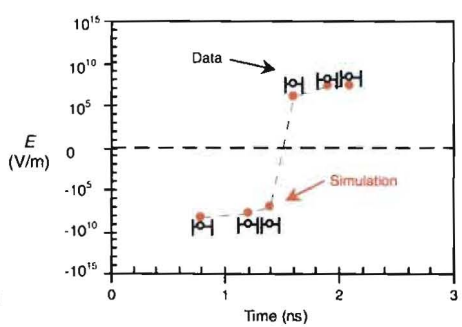

The data is largely consistent with LILAC simulations, and gradient scale lengths for electric potential on the order of 1 micron during inward shock and 100 micron during outward capsule explosion.

Monoenergetic-Proton-Radiography Measurements of Implosion Dynamics in Direct-Drive Inertial-Confinement Fusion, C. K. Li *et al.*, Phys. Rev. Lett. **100**, 225001 (2008)

Another example: charged-particle radiography in asymmetric ICF implosion

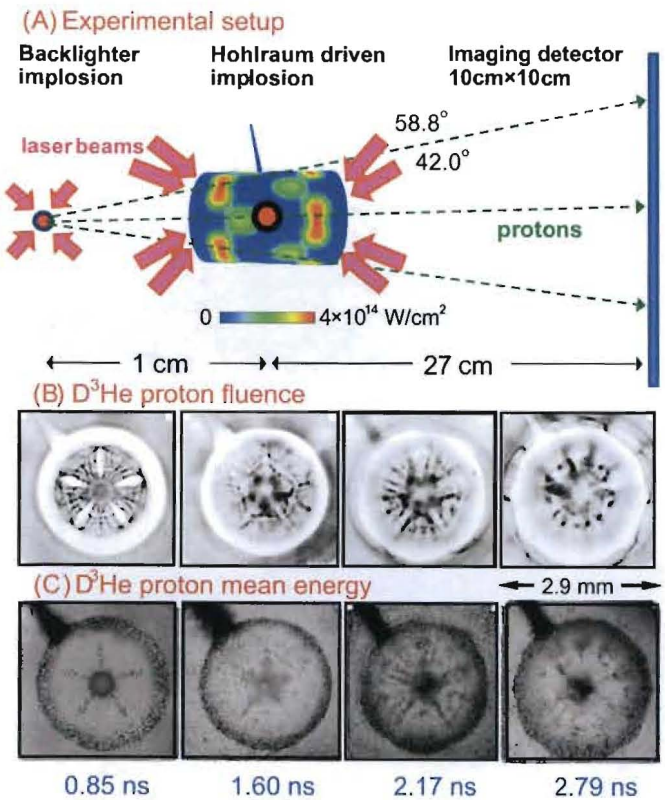

Results from Li, Petrasso, et.al., (Sciencexpress, Jan.28, 2010). The authors rule out B field as source by symmetry arguments.

- Asymmetries can be related to generation of B through Faradays law: $dB/dt \sim -\nabla \times E$
- B is expected to move with fluid (interfaces) and dissipation is small above a few hundred eV.
- Charged particle radiography can potentially detect the large B, and thus the interface.
- Our preliminary estimates suggest asymmetries and therefore B may be more important than E.
- Li, Petrasso, et.al., rule out B deflections in this work due to 'symmetry' arguments.
- eBeam radiography may prove useful to resolve apparent discrepency.

Motivation: can E & B in plasma applications be ignored in hydrodynamic simuations ?

- Laser-matter plasma
  - E & B are 'well-known' here and studied for > 30 yrs
- Omega scale ICF
  - E & B observed in recent studies (Li, Petrasso, et.al., 2008-2010)
  - Charged particle (CP) diagnostics
- NIF scale ICF
  - E & B expected in NIF regime
  - Will require higher rho-r access than in previous CP diagnostics
- HEDP experiments
  - E & B possible explanations in transient plasma regimes (e.g., U. Mich. experiments)

To what extent are these plasmas so dense that it is justified to treat them as hydrodynamic fluids as in many plasma fluid simulations ?

eBeam Radiography for plasma and HEDP experiment diagnostics: physics summary

- Confined plasma produces radial E
  - Simplified Ohm's Law with small J and B
- Asymmetries in E (thru implosion asymmetries) generate dB/dt.
  - Faraday's Law
  - B moves with and thus accumulates with plasma motion and with negligible dissipation at T > ~ 500eV
- Charged particle (electron) radiography can potentially detect:
  - The density variations, rho-r, including densities in NIF
  - The large E field (related to shock fronts)
  - the large B field (related to plasma material interfaces).
- Distinguishing eBeam deflection signals from MCS (multiple Coulomb scatter proportional to rho-r) and from E and B is a focus of this study.
  - Detailed forward calculations and analysis needed
  - E and B in plasma, eBeam transport thru plasma, eBeam thru radiography imaging system.
- Analysis is key to design basis for the eBeam lens-collimator-imaging system.

Benefits of electron radiography for plasma and HED object diagnostics

- Greater access to high rho-r regimes in plasma or solid (30 Mev electrons range up to ~ 10 g/cm2)
  - Range of 30 MeV electron deflection is several times greater than 15 MeV protons
  - Needed in NIF-like regimes
  - Full range of plasma density regimes accessible
- Greater sensitivity to deflecting E or B fields
  - 30 MeV electron deflection is several times greater than 15 MeV protons
- Compact, off-the-shelf, sources
  - S-band (2-4 GHz) RF accelerator technology for low energy electron beam generation has been extensively developed for medical applications
    (*Medical Electron Accelerators*, C. J. Karzmark, C. S. Nunan, E. Tanabe, McGraw-Hill, 1993)
  - No need to divert laser power to create charged particle source
  - 'semi-portable' - setup in field at plasma experiment
- Multiple time-sequence radiographs in a single test
  - Compact accelerator provides a pulse-train of electrons
  - Fast gating to minimize motion blurr
- Collimated source allows use of angular collimation imaging optics
  - Technique used at LANSCE pRad (as opposed to point-projection used in proton imaging)
  - Improved spatial and temporal resolution? (TBD)

Deflection signal: eRad vs.pRad

Improvement with the proposed 30 MeV electrons over 15 MeV protons.

- Sample calcs
- Plasma conditions as expected in Trident laser-foil experiment
- Te ~ 600 eV
- n_e ~ 2e20 cm^{-3}
- Size ~ 1mm x 200 um
- Time ~ 1 ns
- eBeam advantage expected to be greater in denser plasma.

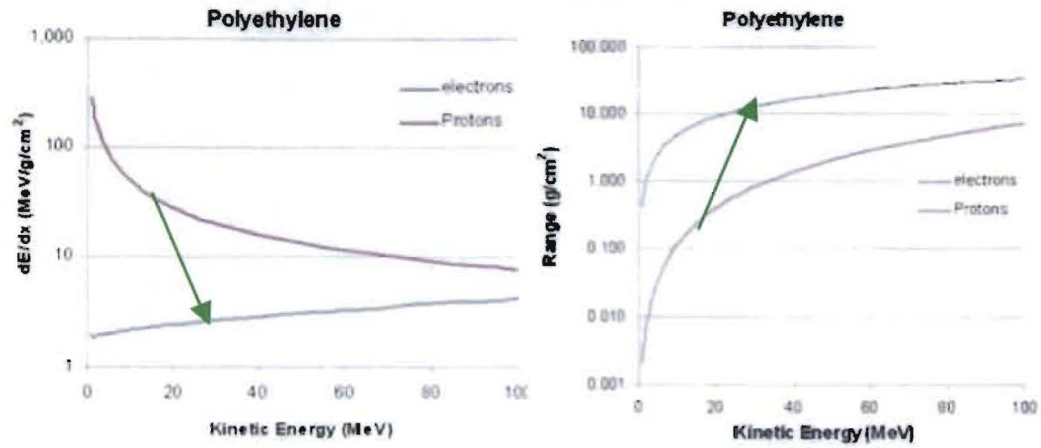

Left: dE/dx in polyethylene for electrons and protons as a function of energy. Right: range of protons and electrons as a function of energy. From this comparison it is clear that moderate energy electrons are better suited for radiography of thicker dynamic systems.

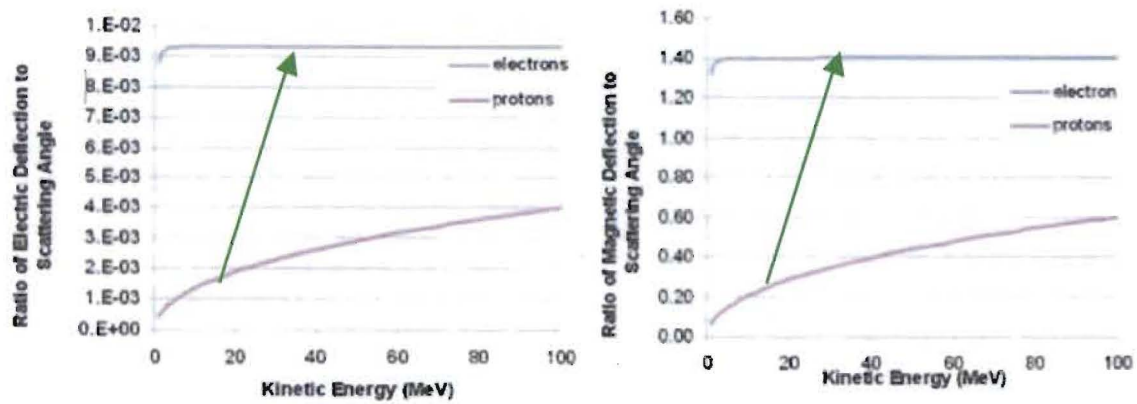

Left: ratio of deflections due to electric fields divided by multiple Coulomb scattering deflections. Right: ratio of deflections due to magnetic fields divided by multiple coulomb scattering deflections. From this comparison it is clear that moderate energy electrons are better suited than protons for measuring E and B fields.

A collaboration between LANL and Idaho Accelerator Center (IAC) demonstrated rho-r discrimination using eRad on static objects in 2005

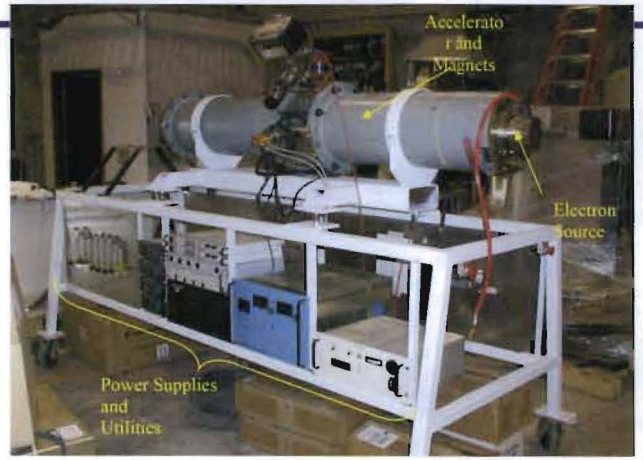

Commercial electron accelerator, ~ 2 m long, 5-30 MeV, 2.8 GHz, 120 mA, ~ 100 ps long pulses of > 10^{10} electrons/pulse separated by 357 ps over a total duration of 2 μs installed on a transportable frame at IAC

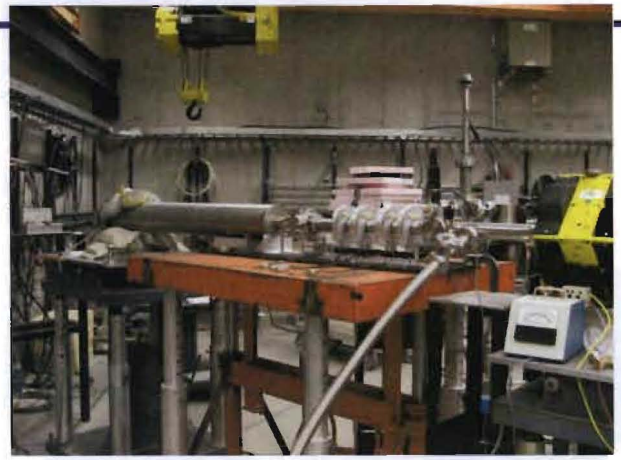

Imaging system based on permanent magnifier quadrupoles used in demonstration experiments

- Preliminary design of an imaging lens indicates a resolution of ~ 10 μm with a few mm field-of-view and a total length of ~ 1 m from the object to the image plane
- current proposal refines concept and requirements
- A proposal to build and test eRad prototype on HED objects has been submitted

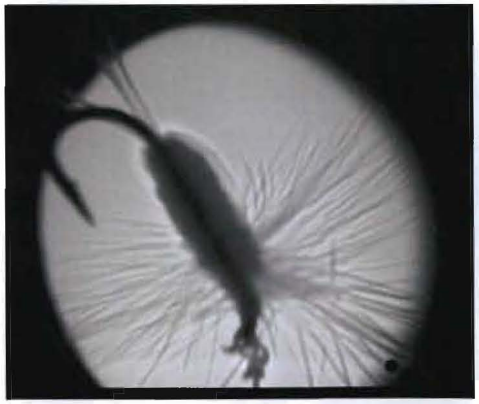

Electron radiograph of familiar object collected with the demonstration system

Portable Electron Radiography System, F. E. Merrill *et al.*, Proceedings of Particle Accelerator Conference, 2005
Electron Radiography, F. E. Merrill *et al.*, NIM B **261**, pp. 382–386 (2007)

eRad = eBeam Radiography

Investigations to include:
- Distinguish E, B and rho-r
- Resolution vs rho-r, E, B
- Lens-collimator-image design optimizations

Electron accelerator

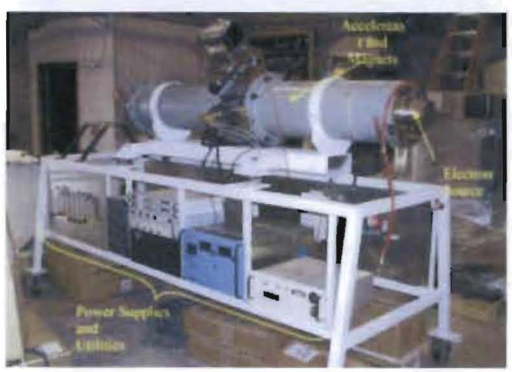

Plasma test object

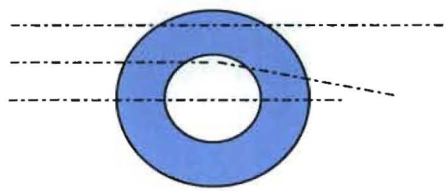

f[x] or f[θ]

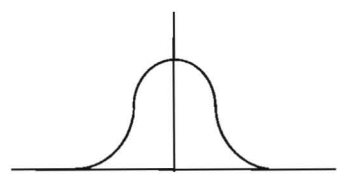

Electron imaging system

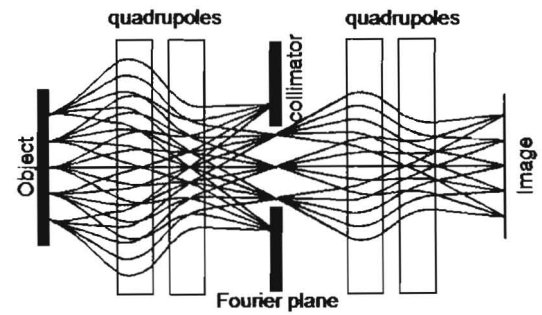

- Estimate E, B and rho in object
- eBeam transport thru object
  - f[x, θ] exiting plasma
- eBeam transport thru lens-collimator-imaging system
- Signals in image plane:
  - Electron fluence
  - Electron energy

eBeam Radiography Forward Calc

- Compute 2-D plasma / fluid solution for object in cylindrical (r,z) coordinates.
- Estimate E and B from plasma fluid solution (small **B** and **j** limit).
  - Eventually compute E and B in self-consistent plasma
- Spin cylindrical solution (material, density, E and B) into 3-D object.
- Transport eBeam (30MeV) thru 3-D object.
  - $\mathbf{u}_e \sim u_e \mathbf{x}$
- Accumulate deflections due to MCS (multiple coulomb scatter) and due to E and B deflections at object exit plane, and $(dE/dx)_e$.
- Transport eBeam distribution through eBeam imaging system: magnetic lens, collimator and detection system.
- Optimize eBeam imaging system for resolution in rho-r and/or signal to noise for E/MCS or B/MCS.

E & B in plasma fluids
estimated in a low frequency approximation

- Electron momentum equation reduces to 'Ohm's Law'
  - Radial component dominates any nearly spherical confined plasma
  - Assume **j**, **B** and $\mathbf{u}_i$ small
- Faraday's law generates B in non-uniform E
  - Non-uniform radial electric field generates B
  - B accumulates with plasma motion when dissipation is small (T > ~ 500eV)
- Non-uniform B implies current, j
  - Iterate with Ohm's Law
  - Is ***j x B*** small ?

$$E \approx -\frac{\nabla p_e}{n_e e} + ..\left\{ f[j,u_i,B] \sim 0 \ \ ? \right\}$$

$$\dot{B} \approx -\nabla \times E$$

$$\nabla \times B \approx \mu_o j$$

Implications of eBeam - plasma deflection angle estimates

- Deflection by E
  - Ratio of plasma or test object potential relative to eBeam energy, times the ratio of the transit distance over perpendicular potential gradient scale length.
  - Dominant contribution in plasma expected across shock (smallest gradient scale length).

$$\frac{Du_e[E]}{u_e} \sim -\frac{e\,V}{m_e u_e^2}\frac{d_\parallel}{d_\perp} \sim -\frac{2\,T_e}{E_e}\frac{d_\parallel}{d_\perp}$$

- Deflection by B
  - Is approximately the E deflection modified by a characteristic time for the B field to accumulate in the plasma, τ_B.
  - B accumulates where advected with plasma flow (e.g., at plasma material interfaces but not at shock fronts) and where dissipation is small (T > ~ 500 eV).

$$\frac{Du_e[B]}{u_e} \sim \frac{Du_e[E]}{u_e}\frac{u_e \tau_B}{d_\times}$$

- Deflection by Multiple Coulomb Scatter
  - Scales as a diffusive process, with the square root of the transit distance thru scattering material.
  - Computed as a random walk process on the deterministic deflections by E or B.

$$\frac{Du_e[C_{ei}]}{u_e} \sim \left\langle \Theta^2 \right\rangle^{1/2} \sim \left(2\pi\, n_i \left(\frac{2 z_1 z_2 e^2}{p_e u_e} \right)^2 \ln\left(\frac{b_{\max} + b_{\min}}{b_{\min}} \right) d_\parallel \right)^{1/2}$$

eBeam - plasma deflection magnitudes**

- eBeam deflections

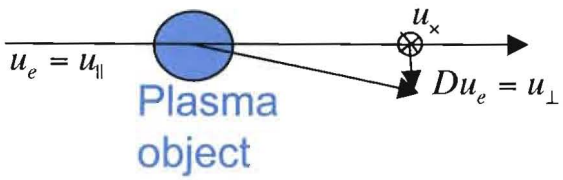

$$m_e n_e \frac{Du_e}{Dt} \sim -n_e e E - n_e e\, u_e \times B - n_e \nu_{ei} u_e$$

$$\frac{Du_e}{Dt} \sim -\frac{e}{m_e} E - \frac{e}{m_e} u_e \times B - \frac{\nu_{ei}}{m_e} u_e \qquad m_e = E_e / u_e^2 \Rightarrow \sim E_e / c^2$$

- E field

$$\frac{Du_e[E]}{u_e} \sim -\frac{e}{m_e u_e} E\, Dt \sim -\frac{e}{m_e u_e} E\, \frac{d_\parallel}{u_e} \sim -\frac{e}{m_e u_e} \frac{V}{d_\perp} \frac{d_\parallel}{u_e} \sim -\frac{e\,V}{m_e u_e^2} \frac{d_\parallel}{d_\perp} \sim -\frac{2\,T_e}{E_e} \frac{d_\parallel}{d_\perp}$$

- B field

$$\frac{Du_e[B]}{u_e} \sim -\frac{e}{m_e u_e} (u_e \times B)\, Dt \sim -\frac{e}{m_e u_e} (u_e \times B)\, \frac{d_\parallel}{u_e} \sim -\frac{e\,(u_e \times B)}{m_e u_e^2} d_\parallel$$

$$\frac{Du_e[B]}{u_e} \sim -\frac{e\,(u_e \times B)}{m_e u_e^2} d_\parallel \sim -\frac{e\,(u_e \times \int \dot{B}\, Dt_B)}{m_e u_e^2} d_\parallel \sim \frac{e\,(u_e \times \int \nabla \times E\, Dt_B)}{m_e u_e^2} d_\parallel \sim \frac{e\left(u_e \times \frac{\tau_B}{d_\times} \frac{V}{d_\perp}\right)}{m_e u_e^2} d_\parallel$$

$$\frac{Du_e[B]}{u_e} \sim \frac{e\left(u_e \times \frac{\tau_B}{d_\times} \frac{V}{d_\perp}\right)}{m_e u_e^2} d_\parallel \sim \frac{e\,V}{m_e u_e^2} \frac{d_\parallel}{d_\perp} \frac{u_e \tau_B}{d_\times} = \frac{Du_e[E]}{u_e} \frac{u_e \tau_B}{d_\times}$$

- Coulomb scatter

$$\frac{Du_e[C_{ei}]}{u_e} \sim \frac{\nu_{ei} m_e u_{e-\perp} Dt}{m_e u_{e-\parallel}} \sim \frac{\nu_{ei} m_e u_{e-\perp} d_\parallel}{m_e u_{e-\parallel}^2} \sim \langle \Theta^2 \rangle^{1/2} \sim \left(2\pi\, n_i \left(\frac{2 z_1 z_2 e^2}{p_e u_e}\right)^2 \ln\left(\frac{b_{max} + b_{min}}{b_{min}}\right) d_\parallel\right)^{1/2}$$

** non-relativistic case shown, similar result for relativistic electrons

eBeam calc. notes: computational representations of MCS (multiple coulomb scatter)

- Gaussian distribution for small angle MCS
- Add rare large angle scatter events per Jackson (classical E)
- Combine as a single probablity function
- Issues w/ discontinuity at small and large angle scattering 'cross-over'

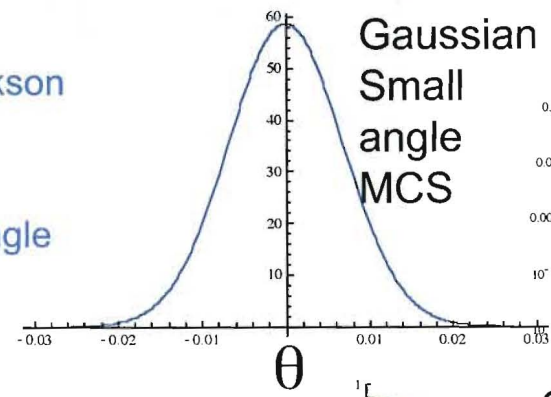

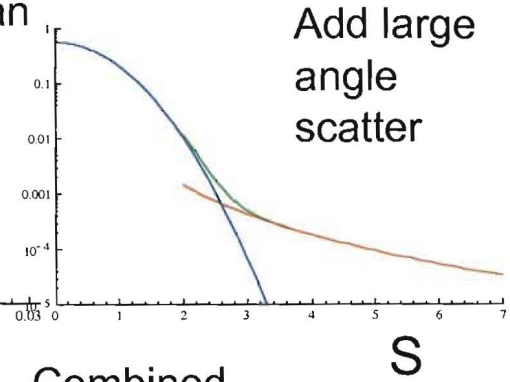

- Issues w/ discontinuity at small and large angle scattering 'cross-over'
  - Dependent upon the value of s = theta/theta-mean chosen to start large angle scattering contribution
- Integrate as cumulative distribution, CDF
- Recover probability as 1 - CDF

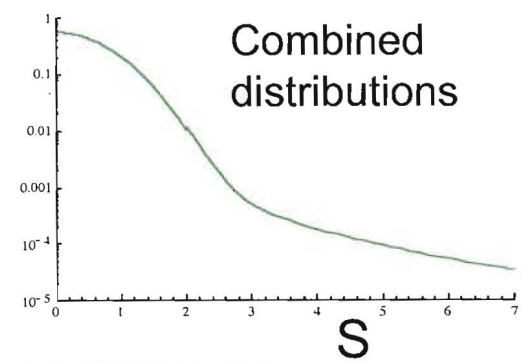

S = scattering angle in units of small angle MCS standard deviations

$$S = \theta/\langle\theta^2\rangle^{1/2} = \theta/\theta_{sd}$$

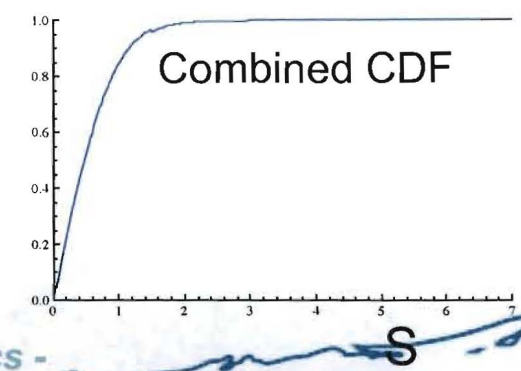

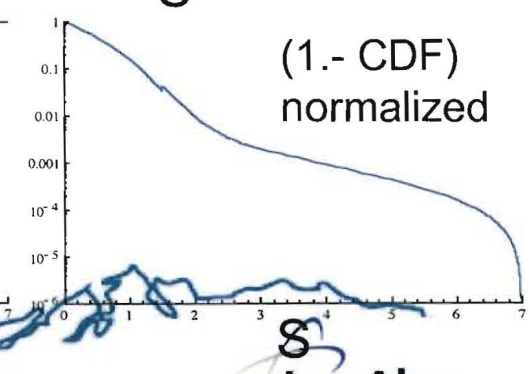

eBeam calc. notes: Forward transport thru plasma feeds into magnetic imaging calculation.

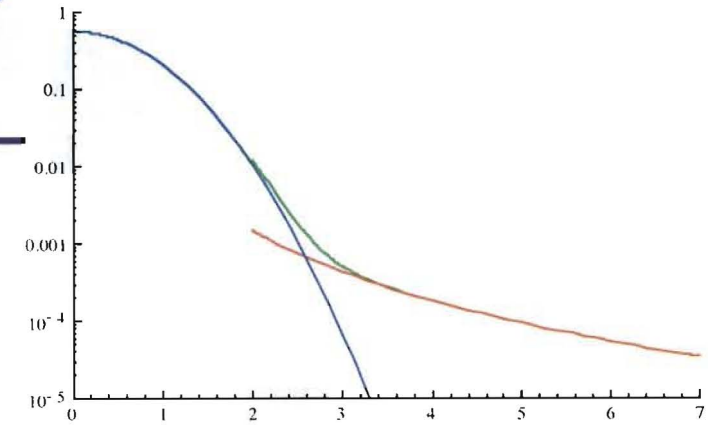

- Gaussian distribution for small angle MCS
- Add rare large angle scatter events per Jackson (classical E)
- Combine as a single probability function

- Scattering distributions recovered from MC random sampling with varying numbers of collisions.
- Samples needed:
  - 10^3 - 10^4 for small angle MCS
  - 10^5 - 10^6 for large angle scattering

- MC will provide basis for eBeam forward transport calculations through more complex test and plasma objects.

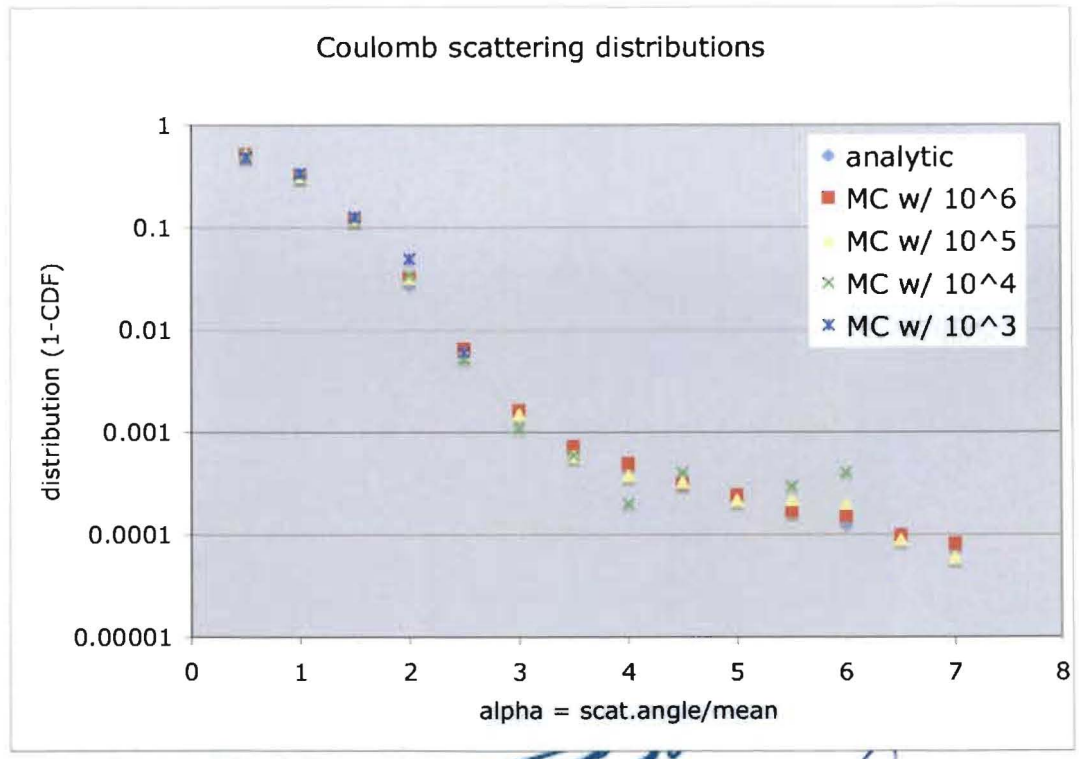

eRad test object 1: Coax cable RG-59 B/U: for developing a forward computational capability

Coax cable sketch

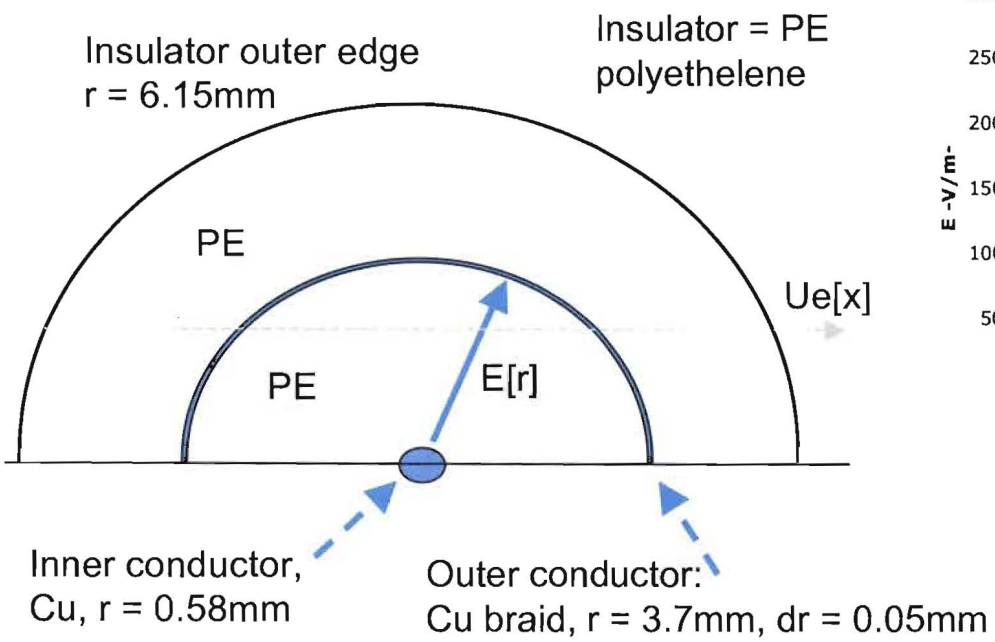

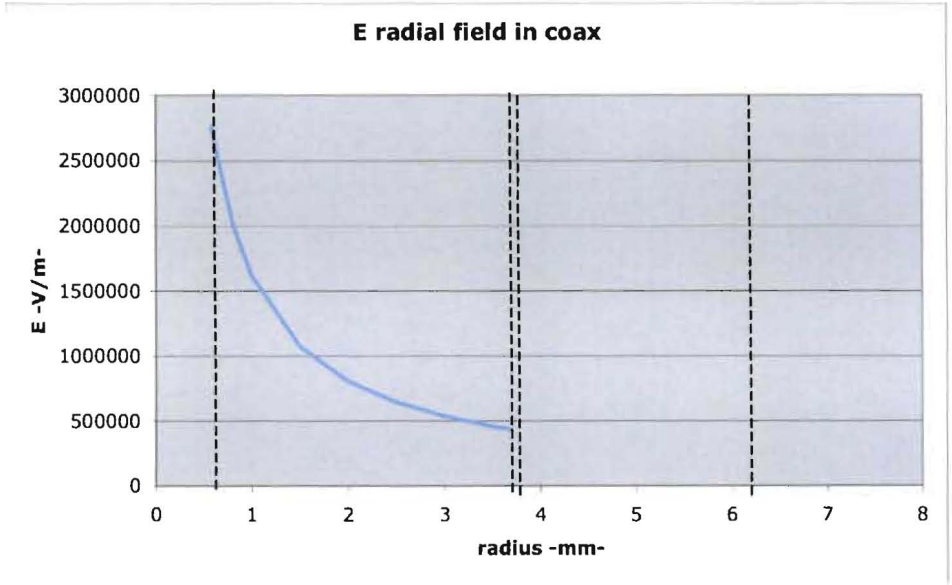

eBeam deflections in coax cable test object due to MCS (multiple Coulomb Scatter) and E[r]

Scattering angle in radians for small angle MCS and for E deflection

- No eBeam collimation
  - $s_{MCS} >> s_E$
- 'wide' eBeam collimation
  - Brings collimated MCS signal closer to E deflection signal
- 'narrow' eBeam collimation
  - Acceptance angle just wide enough to accommodate max deflection due to E

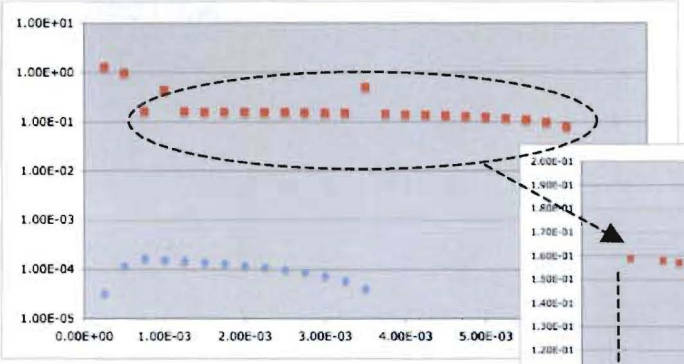

Expanded scale shows expected profile for MCS across coax cable insulation.

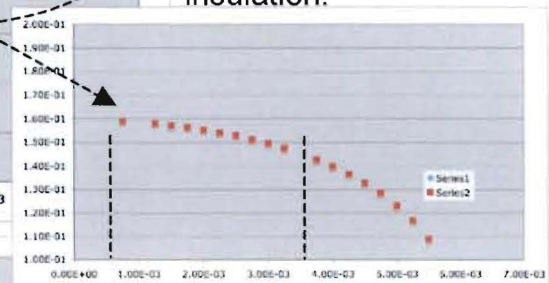

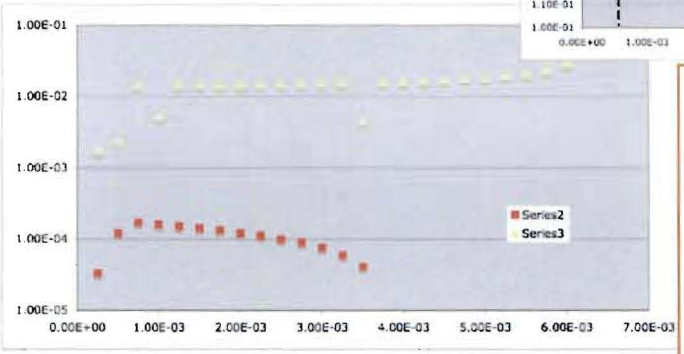

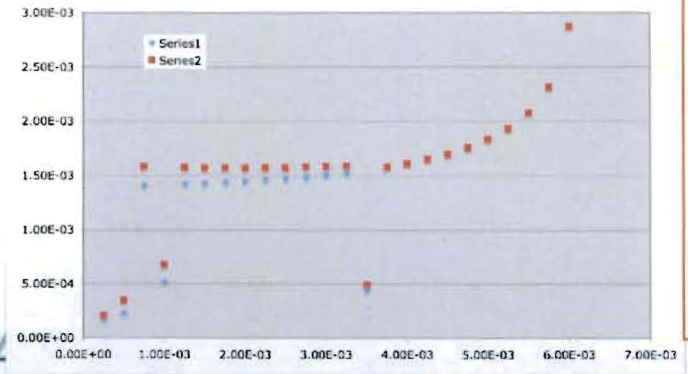

Narrow eBeam is simplest possible magnetic collimation - can bring MCS and E deflections into same range - more sophisticated collimations possible.

Test object 2: concentric sphere of unit density surrounding sphere of density two

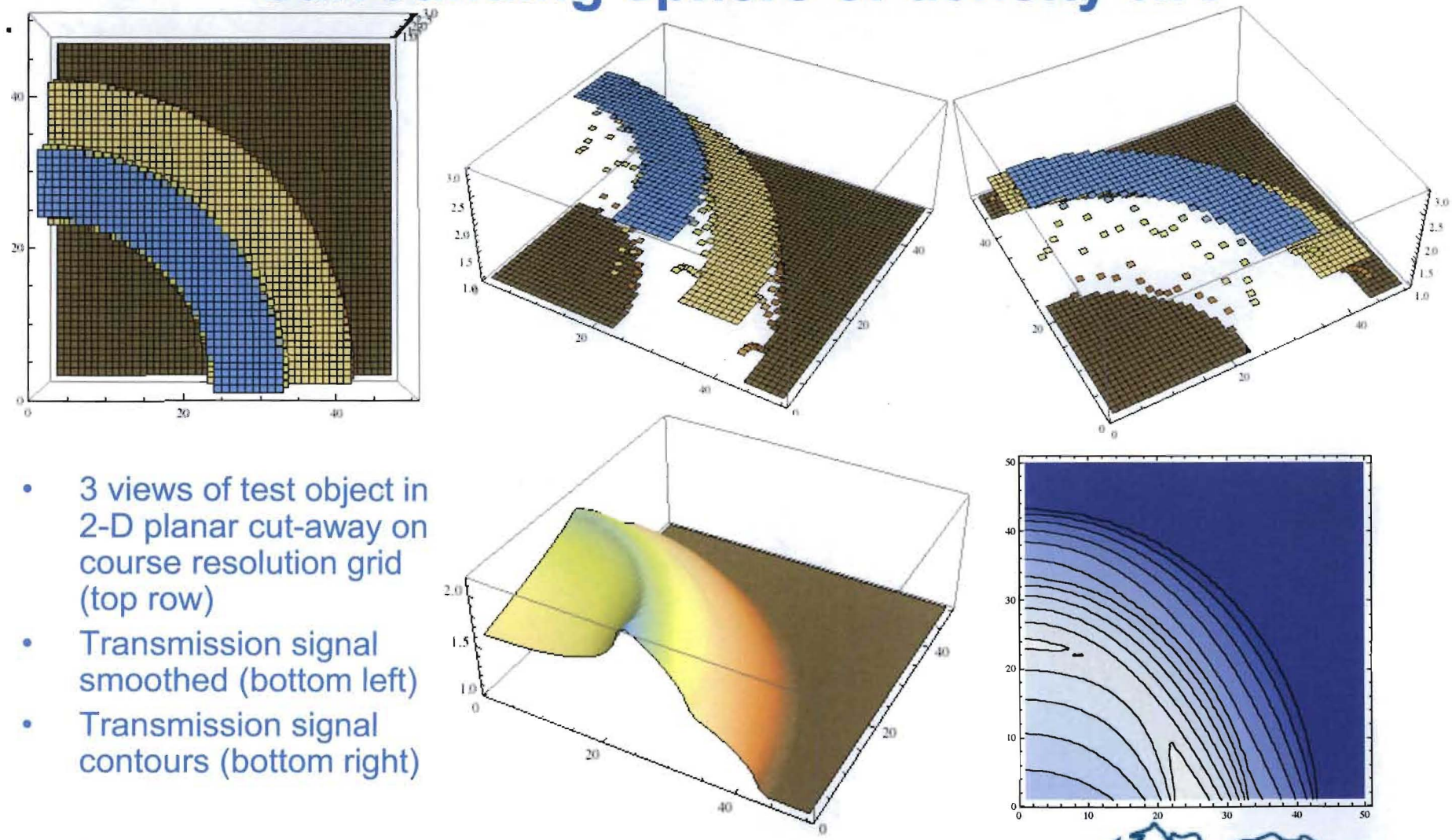

- 3 views of test object in 2-D planar cut-away on course resolution grid (top row)
- Transmission signal smoothed (bottom left)
- Transmission signal contours (bottom right)

Subtle differences in 3-D rotation of 2-D planar solution alter the transmission signal

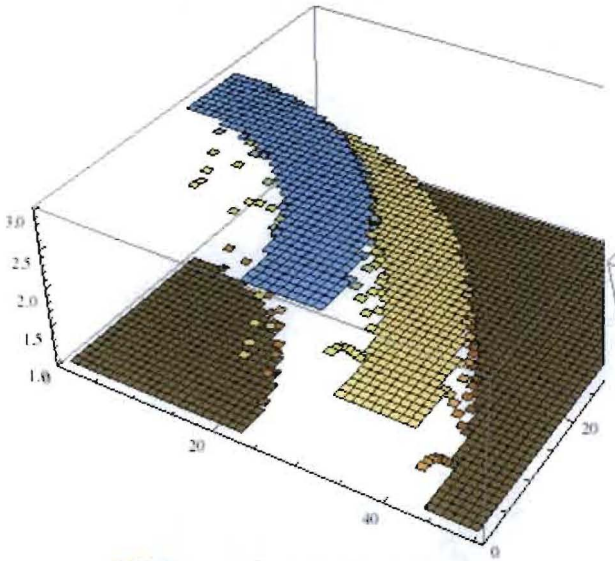

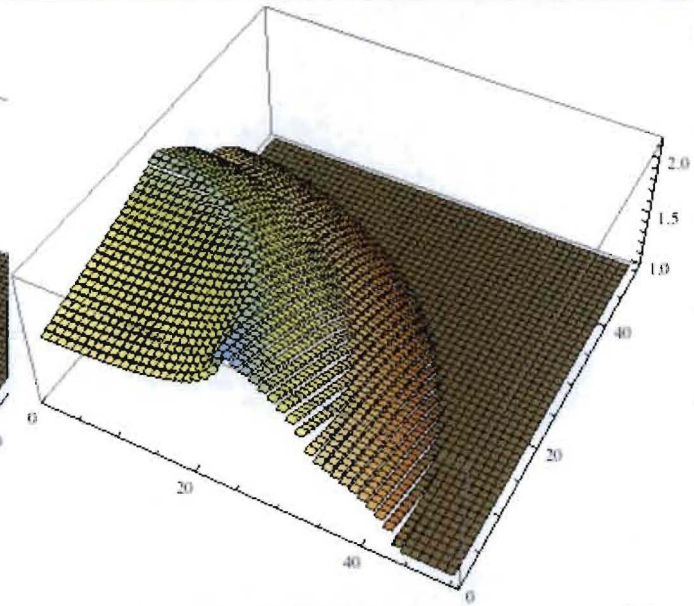

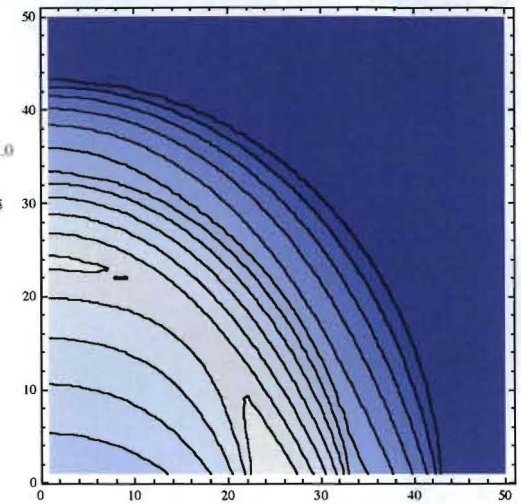

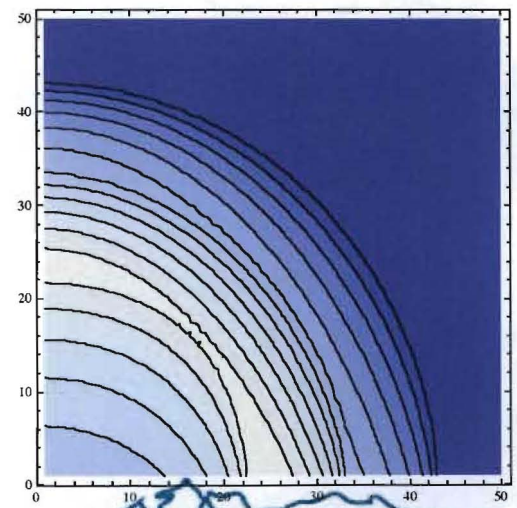

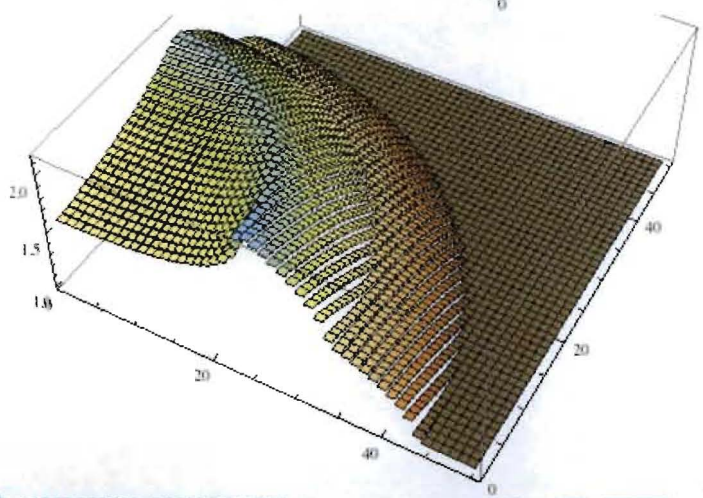

- Object in 2-D plane (above)
- Transmission signals thru two different 3-D rotations (center)
- Contours of the two transmission signals (far right)

Laplacian filtered transmission signals recover object edges.

- Small differences in transmission signal lead to differences in object edges recovered in a simple Laplacian filtering.
- Innermost edge shows the largest discrepancy between the two transmission reconstructions.

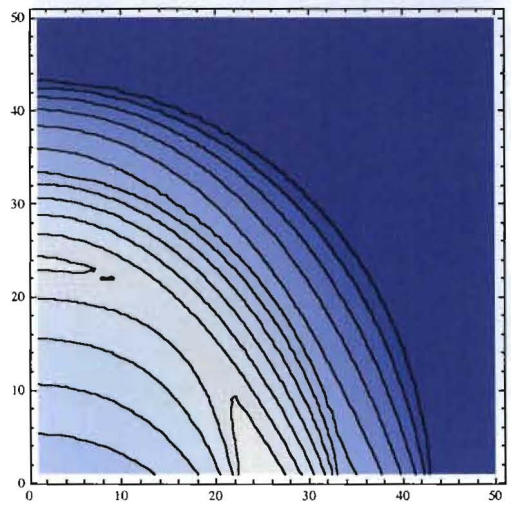

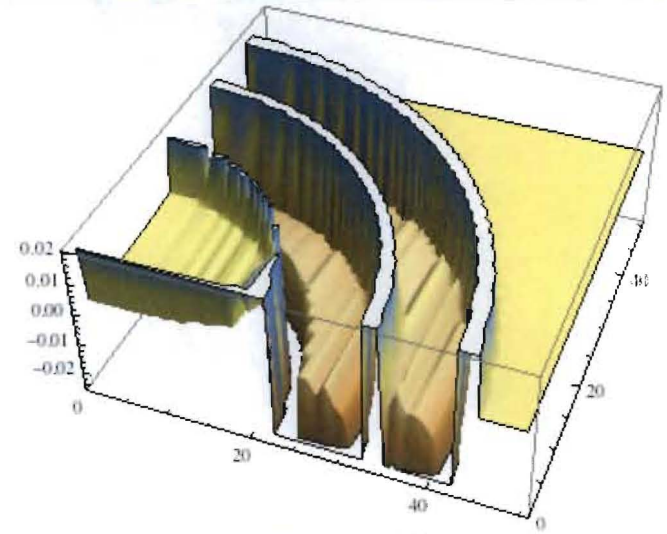

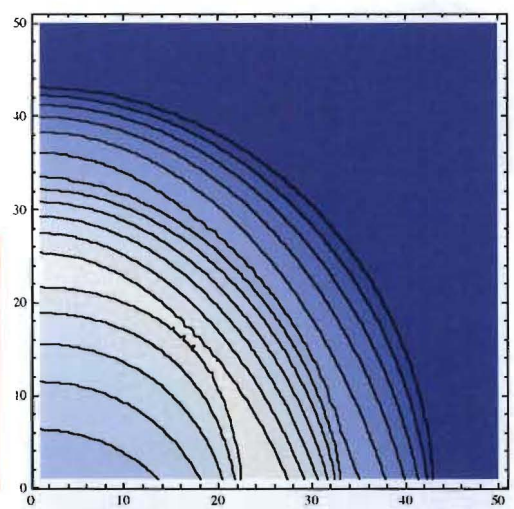

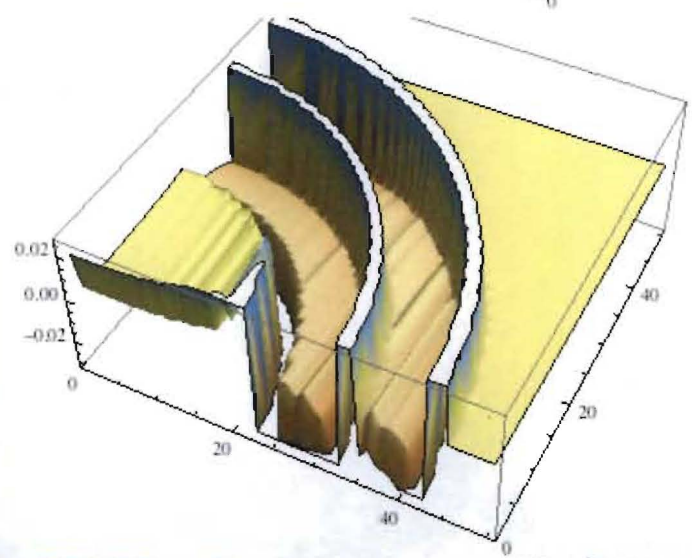

Inner edge is most important in ICF fuel-capsule mix, but is hardest to resolve.

Even in simplified ICF geometry, E & B can become complicated. Plasma fluid vorticity is expected to oppose vorticity on ions due to self-consistent magnetic field and current.

Implosions with density and pressure not exactly aligned.

$$\dot{B} = -\nabla \times E = \nabla \times \frac{\nabla p_e}{n_e e} = -\frac{\nabla n_e \times \nabla p_e}{n_e^2 e}$$

$$E \sim -\frac{\nabla p_e}{n_e e}$$

- Fluid vorticity is assumed to act in same direction on ions.

$$\dot{\omega} \propto \frac{\nabla \rho \times \nabla p}{\rho^2}$$

- Vorticity thru B as curl of electric field, from grad Pe acts in opposite direction on ions.

$$\dot{\omega}_{B \to i} \propto \frac{\nabla p_e \times \nabla n_e}{n_e^2}$$

Fluid implosion

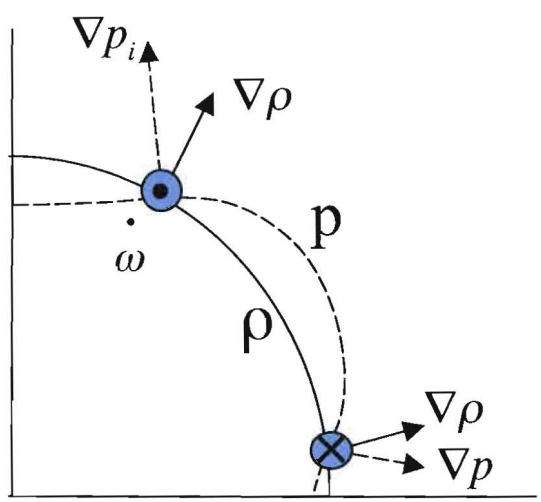

Vorticity during inward moving shock assumed for plasma ions.

Plasma implosion

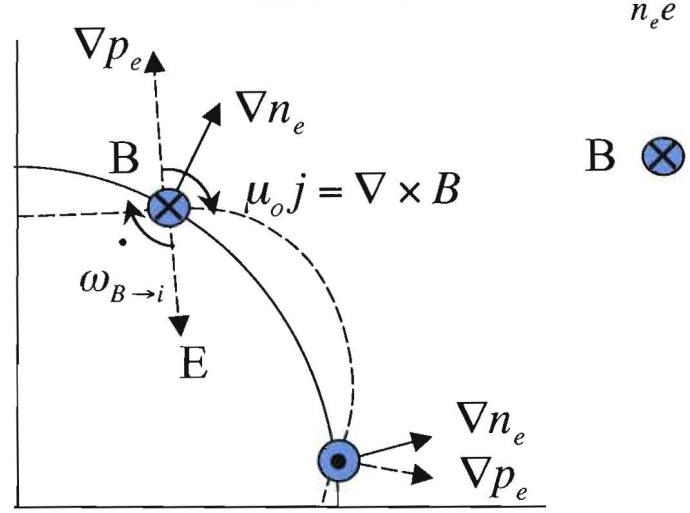

Effective vorticity on ions from B field induced by perturbations of radial E.

Preliminary analysis of 2 fluid plasma shows a magnetic 'vorticity' acts on ions opposite to fluid vorticity thru generated plasma current and ion-electron collisions.

The eRad diagnostic could benefit a broad range of NIF, Omega and Trident plasma experiments AND non-plasma HED experiments.

- Multi-frame (~5-10) radiography in a single experimental shot
- Possibility of detecting locations of shocks and complex interfacial mixing structures in a plasma fuel region
- An estimate for eRad development path will require several steps:

FY11 - refine concept and requirements

FY12 - field prototype at "small" laser facility (*e.g.*, Trident) to validate concept and requirements

FY13 - design ICF / NIF version

FY14 - purchase NIF eRad hardware & begin assembly, approvals, reviews, etc.

FY15 - finish assembly & demonstrate functionality at NIF

E and B Fields in Plasma Mixing

- Diagnostic signature
  - E and B in plasmas may offer means to interrogate small scale plasma mixing structures
  - Exciting recent work using pRad in ICF
    - (Li, Petrasso, et.al., MIT, Omega, etc.)
  - Charged particle radiography with electron beam (eRad) is proposed to improve diagnostics in several respects:
    - Multiple image per shot, independent power source, 'semi-portable' expected high resolution at high rho-r, and improved sensitivity to E and B
- Role in improving understanding of plasma transport
  - Plasma E and B may modify transport from single fluid Eulerian predictions often applied in ICF and in HEDP
  - E and B depend upon smallest local gradient scale lengths
  - Plasma diffusion must be important at smallest scales - what are these scales in a given experiment ?

Back up slides for discussion and notes to self.

Increasing levels of plasma physics in CFD 'fluid'

- Single fluid
  - Inviscid Euler equations
  - With viscosity -> Navier-Stokes => single fluid DNS
- Multi-fluids inviscid
  - Mass average velocity, VOF, high order advection, LES, iLES, and/or numerical mixing
  - Mix models
    - single fluid turbulence defines species diffusivity
    - mix models based on species velocity (drift flux)
- Multi-fluids w/ molecular diffusion
  - 'variable density' fluids with species fraction equation(s) and 'diffusion flux' - DNS
- Multi-fluids w/ plasma diffusion
  - Modifies multi-fluid diffusion assuming plasma collision times
- Multi-component (u_i, u_e, E, B) plasmas
  - One fluid species coupled with Maxwell eqns
- Multi-component multi-species plasmas
  - With diffusive mass mixing
  - With full species momentum

Areas of interest

- Kinetic and MD approaches
  - Boltzmann transport eqn, PDFs, non-Maxwellian, averaged collision operators…
  - MD models collision / particle interaction process explicitly

Kinetic theory leads from Boltzmann equation to single fluid or to single species plasma moment equations

Kinetic

$$\frac{D f_i[x,v,t]}{Dt} = \frac{\partial f_i}{\partial t} + v\frac{\partial f_i}{\partial x} + a\frac{\partial f_i}{\partial v} = C_{i-j}$$

$a = q_i/M_i(E + u \times B)$

$f_i \sim f_i^o + f_i^1$
- f_i^o -> drifting Maxwellian
- f_i^1 -> 'closure'-> flux ~ grad(moments)

Velocity 'moments' of the distribution function

$$\rho_i = m_i \int (f_i[v_i])dv_i$$
$$\rho_i u_i = m_i \int (f_i[v_i])v_i dv_i$$
$$E_i = \rho_i u_i u_i = m_i \int (f_i[v_i])v_i v_i dv_i$$

Single fluid

ρ
ρu
$\rho(\varepsilon+u^2/2)$

Conservation of velocity 'moments'

Single species plasma - ions and electrons w/ [E, B]

ρ_i	ρ_e
ρu_i	ρu_e
$\rho(\varepsilon+u^2/2)_i$	$\rho(\varepsilon+u^2/2)_e$

$p = \mathrm{trace}(P) = \mathrm{trace}(n_i v_i v_i)$

With Maxwell's equations for [E, B]:

Curl(B), Curl(E)
Div(B), Div(E)

Momentum in a fluid verses single ion species plasma

Kinetic

Single fluid

Consider momentum equation

$$\rho\left(\frac{\partial u}{\partial t}+\nabla\frac{u^2}{2}-u\times\omega\right)=-\nabla p$$

And vorticity

$$\nabla\times\frac{Du}{Dt}=\frac{D\omega}{Dt}=\frac{\partial\omega}{\partial t}-\nabla\times(u\times\omega)\;=\;-\nabla\times\frac{\nabla p}{\rho}=\frac{\nabla\rho\times\nabla p}{\rho^2}$$

Note that sign of baroclinic fluid vorticity opposes 'vorticity' of the magnetic induction.

Combining in the ion equation:

- electric field adds grad(electron pressure)
- fluid vorticity opposes 'magnetic induction vorticity'.

Single species plasma w/ [E, B]

$$\rho_i\frac{Du_i}{Dt}=\rho_i\left(\frac{\partial u_i}{\partial t}+\nabla\frac{u_i^2}{2}-u_i\times\omega_i\right)=-\nabla p_i+n_iz_ie(E+u_i\times B)+\rho_{ie}\nu_{ie}(u_e-u_i)$$

$$\rho_e\frac{Du_e}{Dt}=\rho_e\left(\frac{\partial u_e}{\partial t}+\nabla\frac{u_e^2}{2}-u_e\times\omega_e\right)=-\nabla p_e-n_ee(E+u_e\times B)-\rho_{ie}\nu_{ie}(u_e-u_i)$$

Electron eqn. w/ $(m_e/m_i)\sim 0$, $j\sim 0$, $B\sim 0$, ==>>

$$E\sim-\frac{\nabla p_e}{n_ee}\qquad E\sim-\nabla\phi\sim-\frac{\nabla n_eT_e}{n_ee}\sim\frac{2\,T_e}{L_e}$$

Faraday's Law ==>>

$$\dot{B}=-\nabla\times E$$

Combining ==>>

$$\dot{B}=\nabla\times\frac{\nabla p_e}{n_ee}=-\frac{\nabla n_e\times\nabla p_e}{n_e^2e}$$

$$\rho_i\left(\frac{\partial u_i}{\partial t}+\nabla\frac{u_i^2}{2}-u_i\times\omega_i-\frac{n_iz_ie}{\rho_i}(u_i\times B)\right)=-\nabla p_i-\frac{n_iz_i}{n_e}\nabla p_e$$

Fluid vorticity sources in asymmetric ICF compression
(for assumption of higher density pusher on lower density fuel)

- ⊙ positive vorticity
- ⊗ negative vorticity

- Low mode asymmetry
- Single mode perturbation in quadrant
- Vorticity sources from right-hand rule w/

$$\dot{\omega} \propto \frac{\nabla\rho \times \nabla p}{\rho^2}$$

Inward moving shock

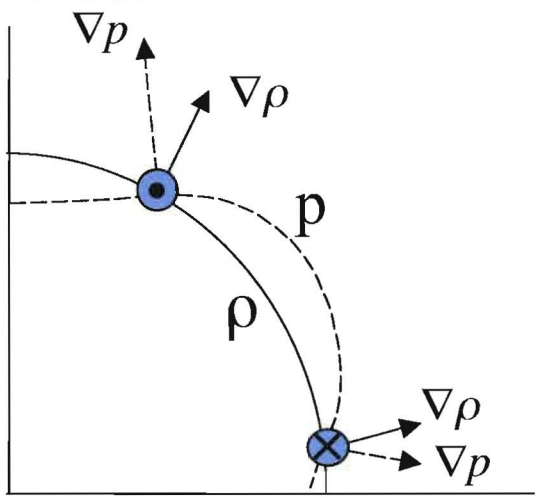

Outward shock from vertical axis adds to inward shock vorticity, and subtracts from more distant source.

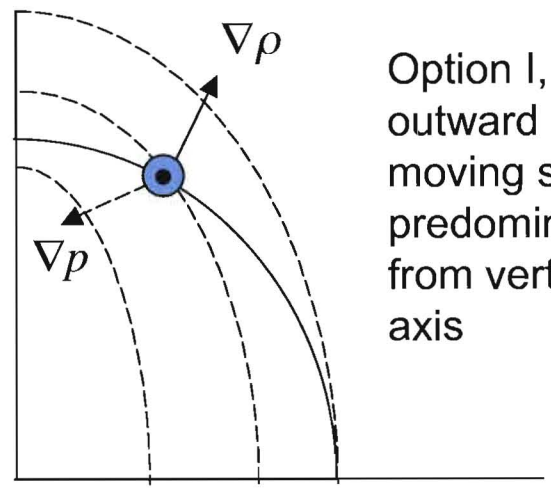

Option I, outward moving shock predominantly from vertical axis

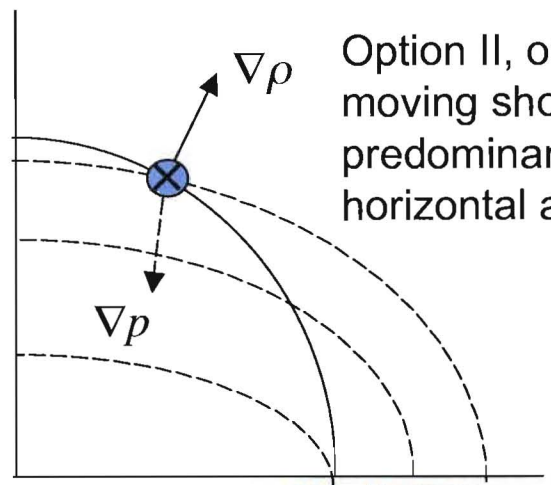

Option II, outward moving shock, predominantly from horizontal axis

Proton Radiography of Inertial Confinement Fusion Implosions

J. R. Rygg, et.al. Science, 319(5867) p.1223, 2008**.

Setup of experiment:

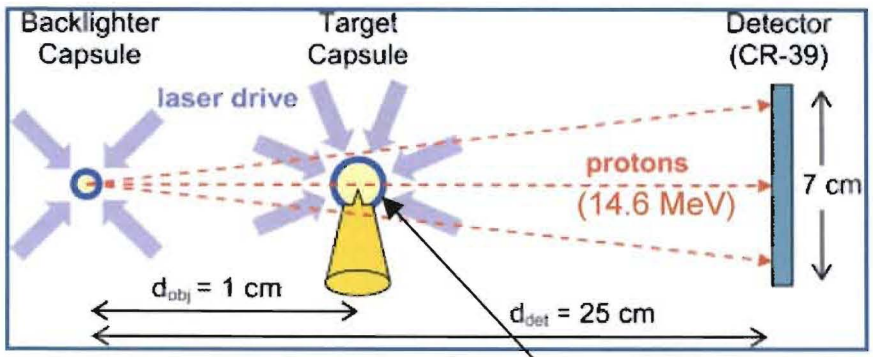

Field of view at object is ~ 3 mm.

Drive pulse is 40 lasers => 5 / octant

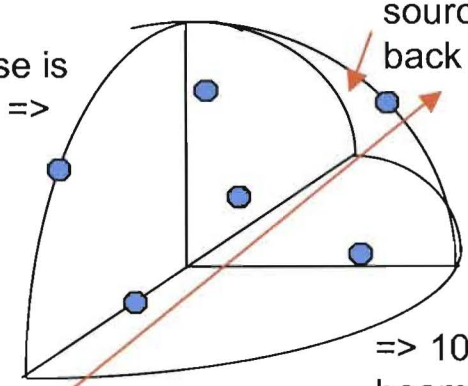

5 more laser sources in back octant

=> 10 drive beams thru quadrant

Line of sight

Dynamic evolution of experiment:

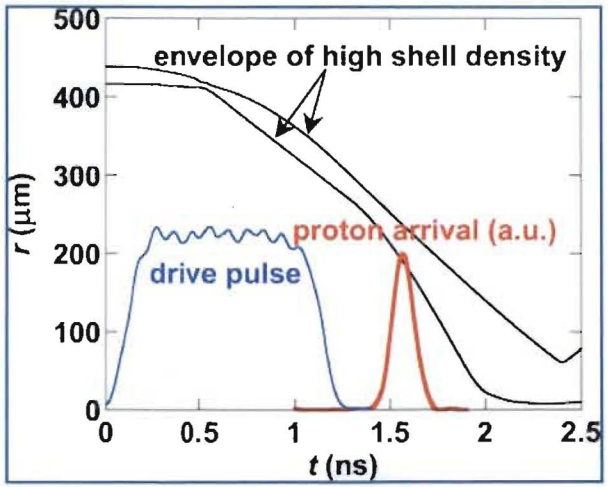

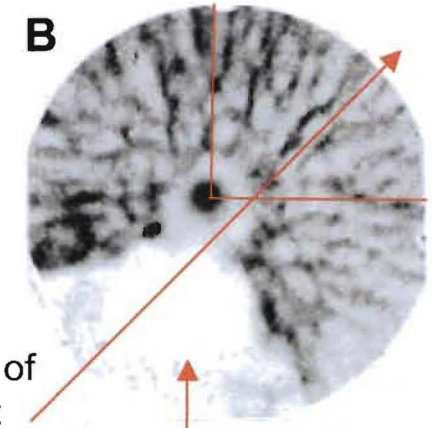

Line of sight

4 lasers => off in 'dome'

Results of experiment interpreted as: large E and B fields determine detector image.

** Proton Radiography of Inertial Fusion Implosions
J. R. Rygg, F. H. Séguin, C. K. Li, J. A. Frenje, M. J.-E. Manuel, R. D. Petrasso, R. Betti, J. A. Delettrez, O. V. Gotchev, J. P. Knauer, D. D. Meyerhofer, F. J. Marshall, C. Stoeckl, W. Theobald
Science 29 February 2008:
Vol. 319, no. 5867, pp. 1223 - 1225
DOI: 10.1126/science.1152640

pRad in ICF interrogates E in a 'nearly symmetric' ICF capsule.

from - C.K. Li, et.al. Phys.Rev.Lett. **100**, 225001 (2008)

pRad image results

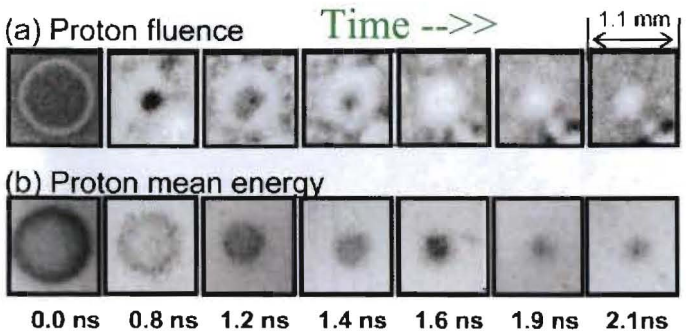

FIG. 2. 15.1-MeV proton radiographs of imploding capsules at different times, illustrating the time evolution of mass distribution and of a previously unobserved radial electric field. In the fluence images (a), darker means higher fluence, while in the energy images (b) darker means lower proton energy (more matter traversed). The gray-scale mapping is different for each image, to account for different backlighter yields (see Fig. 3) and make the most important structure clearly visible.

Results are consistent with:
T [inward shock] ~ 100 eV
T [outward shock] ~ 600 eV

1-D simulation results

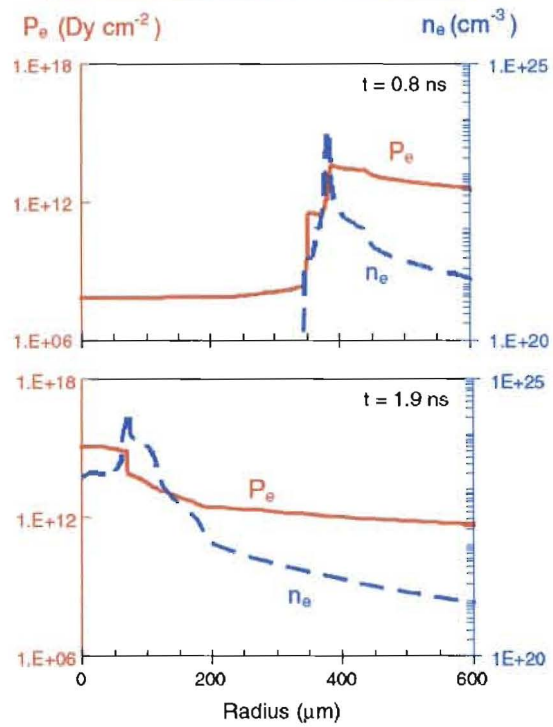

FIG. 4 (color online). Profiles of electron pressure (solid lines) and density (dashed lines) at 0.8 and 1.9 ns, calculated by LILAC.

Inferred E results: comparison of exper. and sims

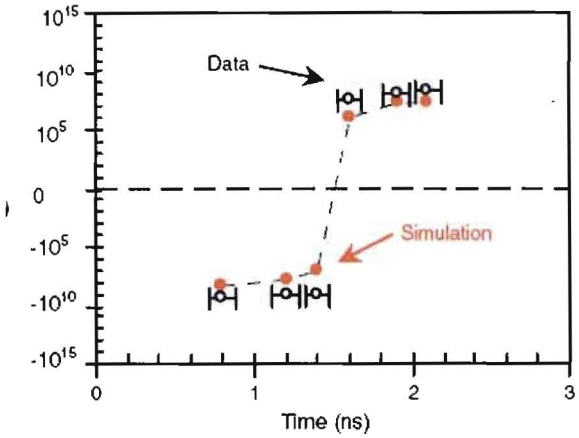

(color online). Radial E fields estimated from experi- measurements (open circles) and from LILAC simula- solid circles) vs implosions times. Horizontal error bars ent uncertainties in backlighter burn time. Vertical error re about the size of the symbols.

Results are consistent with:
eE ~ Te/L w/
L [inward shock] ~1 micron
L [outward shock] ~ 100 micron

Comparison of simulation to laser driven plasma experiment shows 'vorticity' differences.

Figures courtesy of:
Bruce Fryxell, et.al. U. Mich.
A. Budde, C.C. Kuranz, R.P. Drake, M. Grosskopf, C. Krauland, D. Marion, J. Knauer, D. Arnett, C. Meakin, T. Plewa, N. Hearn

Sponsored by: DOE NNSA under the Predictive Science Academic Alliance Program

Laser driven shock from left.

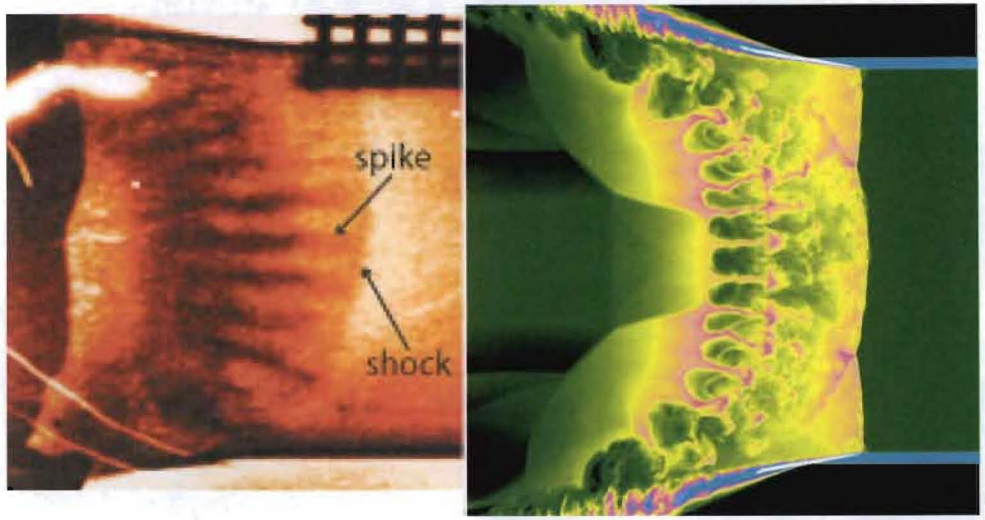

Experiment **3D FLASH simulation**

U. Mich team proposes:
B-fields wrap around individual spikes and bubbles laterally confining the spike and suppressing the mushroom cap formation.

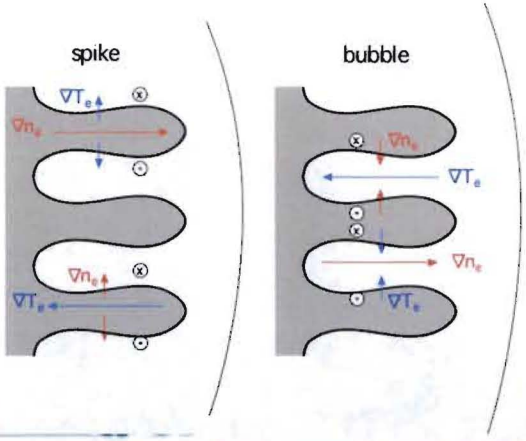

Alternatively, [in my preliminary estimate] …. magnetically induced vorticity sources may cancel usual fluid baroclinic vorticity sources.

E field in a plasma fluid:
options to obtain E from fluid and Maxwell eqns.

- Plasma as a single fluid assumes E (j ~ 0) is related to grad(p_e):

$$f_i \sim -\nabla p_i + n_i q_i E \sim -\nabla p_i - n_i q_i \nabla p_e /(n_e e) \xrightarrow{1_species} -\nabla p_i - \nabla p_e = -\nabla p$$

$$E \sim -\nabla p_e /(n_e e) \sim T_e / L_e$$

- E field from Maxwell eqns:
  - Poisson $\varepsilon_o \nabla \cdot E = \rho_c = n_i q_i - n_e e$

$$n_i q_i - n_e e \Rightarrow \frac{\delta n}{n} \leq O\left(10^{-12}\right)$$

  - Ampere's Law (w/ displacement J)

$$\mu_o^{-1} \nabla \times B = \frac{\partial(\varepsilon E)}{\partial t} + j$$

$$\mu_o \frac{\partial(\varepsilon E)}{\partial t} \sim \mu_o \frac{\partial(\varepsilon_o E)}{\partial t} \sim \frac{1}{c^2}\frac{\partial(E)}{\partial t} = \nabla \times B - \mu_o j$$

MHD

$$\nabla \times B = \mu_o j$$

- E field from electron fluid eqn:
  - U_e eqn. w/ zero inertia approximation -> MHD

$$\rho_e\left(\frac{\partial u_e}{\partial t} + u_e \cdot \nabla u_e\right) \sim 0 = f_e \sim -\nabla p_e - n_e e E - n_e e\left(u_i - \frac{j}{n_e e}\right) \times B + n_e \nu_{ei} j$$

  - U_e eqn. w/ inertia and divergence free current

$$\rho_e\left(\frac{\partial u_e}{\partial t} + u_e \cdot \nabla u_e\right) - n_e \nu_{ei} j \sim -\nabla p_e - n_e e E - n_e e\left(u_i - \frac{j}{n_e e}\right) \times B$$

$$\rho_c \sim 0 \Rightarrow \frac{\partial \rho_c}{\partial t} + \nabla \cdot j \Rightarrow \nabla \cdot j \sim 0$$

Poisson equation in plasma physics

Which Maxwell equations and plasma fluid equations are needed for a dense short-lived plasma ?

- "Quasi-neutrality"
  - $n_i z_i \sim n_e$ for:
    - $(L > \lambda_{Debye})$
    - λ_{Debye} self-shielding length ($\sim 10^{-10}$m)
  - $(n_i z_i - n_e)/n_e < 1$ for:
    - $(L < \lambda_{Debye})$
  - $E \neq 0$
  - $E \sim T_e/eL \sim$ 1keV/mm

E in a quasi-neutral plasma often determined from a generalized Ohm's law derived from the electron fluid momentum equation:

$$\rho_e \frac{Du_e}{Dt} = \rho_e \left(\frac{\partial u_e}{\partial t} + \nabla \frac{u_e^2}{2} - u_e \times \omega_e \right) = -\nabla p_e - n_e e(E + u_e \times B) - \rho_{ie} \nu_{ie}(u_e - u_i)$$

Electron eqn. w/ $(m_e/m_i) \sim 0$, $j \sim (u_i - u_e) \sim 0$, $B \sim 0$, ==>>

$$E \sim -\frac{\nabla p_e}{n_e e} \qquad E \sim -\nabla\phi \sim -\frac{\nabla n_e T_e}{n_e e} \sim \frac{2\ T_e}{L_e e} \qquad \Rightarrow E[V/m] \sim -\frac{10^3[eV]}{10^{-3}[m]} \sim 10^6$$

Poisson's equation - 'usually' assumed not accurate for E in low-frequency quasi-neutral approximation:

$$\nabla \bullet E \sim -\nabla^2\phi \sim \varepsilon_o^{-1} \sum_{is} n_{is} q_{is} - n_e e \sim e\ (n_{is} z_{is} - n_e)/\varepsilon_o \sim 0$$

$$\Rightarrow \nabla \cdot E[V/m] \sim \frac{1}{L_p}\frac{2T_e}{L_e e} \sim \frac{1}{10^{-3}[m]}\frac{10^3[eV]}{10^{-3}[m]} \sim 10^9 V/m^2$$

$$\Rightarrow \nabla \cdot E[V/m] \sim 10^9 V/m^2 = (e \sim 10^{-19})/(\varepsilon_o = 8.854\ 10^{-12})\delta n$$

$$\Rightarrow \delta n = n_i z_i - n_e \sim 10^{17} m^{-3} \Rightarrow \delta n/n[for\ n\ @\ 1mole/cc] \sim 10^{-13}$$

Poisson's equation - not accurate for E in high density (ICF) applications with large electron pressure gradient driven E fields in quasi-neutral approximation - even in double precision arithmetic.

Momentum and E, B basics in a current-free single ion species plasma

Single species plasma w/ [E, B]

$$\rho_i \frac{Du_i}{Dt} = \rho_i\left(\frac{\partial u_i}{\partial t} + \nabla\frac{u_i^2}{2} - u_i \times \omega_i\right) = -\nabla p_i + n_i z_i e\left(E + u_i \times B\right) + \rho_{ie}\nu_{ie}\left(u_e - u_i\right)$$

$$\rho_e \frac{Du_e}{Dt} = \rho_e\left(\frac{\partial u_e}{\partial t} + \nabla\frac{u_e^2}{2} - u_e \times \omega_e\right) = -\nabla p_e - n_e e\left(E + u_e \times B\right) - \underbrace{\rho_{ie}\nu_{ie}\left(u_e - u_i\right)}_{\sim j}$$

Electron eqn. w/ $(m_e/m_i) \sim 0$, $j \sim 0$, $B \sim 0$:

$$E \sim -\frac{\nabla p_e}{n_e e}$$

Faraday's Law ==>>

$$\dot{B} = -\nabla \times E = \nabla \times \frac{\nabla p_e}{n_e e}$$

Integrating ==>>

$$B = \int \dot{B}\, Dt \sim \nabla \times \frac{\nabla p_e}{n_e e} Dt \sim \frac{2\,\partial_x T_e}{L_y \partial x} Dt$$

Scaling Implications for an asymmetric (θ), approximately spherical, confined plasma ($j \sim 0$, $B_o = 0$) :

$E_r[\theta]$ is a zeroth order quantity.
$B[\phi]$ is a first order quantity.

==>> Scaling:

$$E \sim -\nabla\phi \sim -\frac{\nabla n_e T_e}{n_e e} \sim -\frac{T_e \nabla n_e}{n_e e} - \frac{\nabla T_e}{e} \sim \frac{2\,T_e}{L_e}$$

$$\dot{B}_z \sim \frac{E_x}{L_y} \sim \frac{-\nabla_x \phi}{L_y} \sim \frac{\phi}{L_y L_x} \sim \frac{2\,T_e}{L_y L_x}$$

...in moving frame $\quad U_x \approx \partial x / Dt$

$$B = \int \dot{B}\, Dt \sim \frac{2\,\partial_x T_e}{L_y U_x}$$

E and j if $p_e[t]$

Electron motion:

$$\rho_e \frac{Du_e}{Dt} = \rho_e\left(\frac{\partial u_e}{\partial t} + \nabla\frac{u_e^{\,2}}{2} - u_e \times \omega_e\right) = -\nabla p_e - n_e e\left(E + u_e \times B\right) - \rho_{ie}\nu_{ie}\left(u_e - u_i\right)$$

If $j \sim B \sim 0$: $\quad E \sim -\frac{\nabla p_e}{n_e e}$

But if $d(p_e)/dt \neq 0$, then $p_e = p_e[t] \sim f[dT_e/dt] \sim f[E*RxnRate]$, then $E = E[t]$ $\quad E[t] \sim -\frac{\nabla[p_e[t]]}{n_e[t]e}$

Electric field must evolve to keep up with $p_e[t]$. This evolves by the electron motion (relative to ions) or $j \neq 0$ (with relaxation of j proportional to ion-electron collision time).

If $j \neq 0$: $\quad E \sim -\frac{\nabla p_e}{n_e e} - \frac{\rho_{ie}\nu_{ie}}{n_e e}\left(u_e - u_i\right) \sim -\frac{\nabla p_e}{n_e e} - \eta\, j$

(but $B \sim 0$)

Then electron momentum equation cannot be used to get E and j. => need Poisson eqn.

$$\nabla \cdot E \sim -\nabla^2\phi \sim n_i q_i - n_e e$$

Plasma current, j, is expected to scale as the change in electron pressure with time.